Condensed Matter Physics 2008, Vol. 11, No 3(55), pp. 555–570

CONDENSED MATTER PHYSICS

Longitudinal relaxation of mechanically free KH_2PO_4 type crystals. Piezoelectric resonance and sound attenuation

R.R.Levitskii[1], I.R.Zachek[2], A.P.Moina[1], A.S.Vdovych[1]

[1] Institute for Condensed Matter Physics of the National Academy of Sciences of Ukraine, 1 Svientsitskii Str., 79011 Lviv, Ukraine

[2] Lviv Polytechnic National University, 12 Bandera Str., 79013 Lviv, Ukraine

Received June 5, 2008, in final form July 9, 2008

Within the framework of proton model with taking into account the piezoelectric interaction with the shear strain ε_6, a dynamic dielectric response of KD_2PO_4 type ferroelectrics is considered. Experimentally observed phenomena of crystal clamping by high frequency electric field, piezoelectric resonance and microwave dispersion are described. Ultrasound velocity and attenuation are calculated, peculiarities of their temperature dependence at the Curie points are described. Existence of a cut-off frequency in the frequency dependence of attenuation is predicted.

Key words: *ferroelectrics, piezoelectric resonance*

PACS: *77.22.Ch, 77.22.Gm, 77.65.-j, 77.84.Fa, 77.65.Fs*

1. Introduction

Ferroelectric compounds of the KH_2PO_4 family have been studied for nearly 70 years. Extensive experimental data have been accumulated; several models of the phase transitions in these crystals have been proposed and explored (see [1–14]). At the end of 1960-s, attention of theoretical and experimental studies of the ferroelectric compounds has shifted to the problem of the dynamic phenomena. Investigation of the low-frequency dispersion of their dielectric permittivity provides an important information about mechanisms of the phase transitions or dielectric response of the crystals. Despite the success in constructing a microscopic theory of the KH_2PO_4 family crystals mostly phenomenological models were used in interpreting the experimental data as regards the dynamic characteristics. Such models provide no information about the microscopic nature of the dielectric dispersion and do not allow one to adequately describe the effect of different factors on its temperature and frequency dependencies. This problem has not been solved by the Green functions method or Bloch kinetic equation method [8,9,11,12] either.

Most theoretical works on the relaxation phenomena in KH_2PO_4 family ferroelectrics is based on stochastic Glauber model [16]. For the first time this approach was used to describe relaxational phenomena in KD_2PO_4 in [17], where the main features of longitudinal relaxation were explored within the four-particle cluster approximation in the paraelectric phase in KD_2PO_4. In that work the long-range interactions between deuterons was not taken into account, and the theoretical results were not compared with experiment. Later [18–22] a more sophisticated model of the KD_2PO_4 type ferroelectrics and $ND_4D_2PO_4$ type antiferroelectrics was proposed, in which longitudinal dynamic properties of these crystals were calculated within the four-particle cluster approximation for short-range interactions and mean field approximation for long-range interactions. It was shown [12,15,23–25] that the proposed [18–22] theory permits a satisfactory description of longitudinal relaxation in the KH_2PO_4 type ferroelectrics. An attempt to develop a more consistent theory of the KH_2PO_4 family ferroelectrics within the four-particle cluster approximation with taking into account the tunneling (Ω) was made in [26–28]. The model was not sophisticated enough to com-

pare its results with experimental data for the dynamic characteristics of the crystals. At the same time, in these works the fact of suppression of the dynamic characteristics of KH_2PO_4 type crystals by short-range correlations was established for the first time. Instead of the tunneling frequency, an effective parameter $\tilde{\Omega}$ ($\tilde{\Omega} \ll \Omega$) renormalized by short-range interactions was obtained. It should be noted that the established [26–28] suppression explains, most likely, the Debye character of dispersion of the dielectric permittivity observed in these crystals.

It should be stressed that the ferroelectrics of the KH_2PO_4 family are also piezoelectric. The piezoelectric coupling is revealed particularly when the crystals are subjected to external electric fields and mechanical stresses of certain symmetry. At the ferroelectric phase transition in the KH_2PO_4 type crystals, a spontaneous strain arises which changes their tetragonal symmetry.

Studies of the piezoelectric coupling effect on the phase transition and on physical properties of the KH_2PO_4 type ferroelectrics were initiated in [29], where the Slater model [30] was modified by taking into account the splitting of the lowest ferroelectric level by the strain ε_6.

Fundamental are the results obtained in [31,32], where the proton ordering model was modified for the first time by taking into account the deformational molecular field related to the strain ε_6 as well as the splitting of "lateral" deuteron configurations. In [33,34], with taking into account all possible splittings of configurational energies ("upper/lower", "lateral", and single-ionized configurations) due to the strain ε_6, the phase transition and the effect of the stress σ_6 [33] and field E_3 [34] on the physical characteristics of $K(H_{0,12}D_{0,88})_2PO_4$ crystals were explored. Tunneling was not taken into account. A satisfactory agreement of theoretical results and experimental data was obtained.

Physical characteristics of the KH_2PO_4 family crystals with taking into account piezoelectric coupling and tunneling are explored theoretically in [35].

So far the model consideration of longitudinal dielectric characteristics of the KD_2PO_4 type ferroelectrics has been restricted to the static limit and to the microwave region [15,18–25]. Attempts to explore the piezoelectric resonance phenomenon within a model that does not take into account the piezoelectric coupling are pointless. Conventional proton ordering model of the KD_2PO_4 type ferroelectrics does not permit one to describe the effects related to the difference between the free and clamped regimes or the phenomenon of crystal clamping by high-frequency electric field.

It seems natural to calculate, within the proposed in [33] proton ordering model with piezoelectric coupling, the dynamic characteristics of the KD_2PO_4 type ferroelectrics in a wide frequency range from 10^3 Hz to 10^{12} Hz, including the piezoelectric resonance region. In [36] within the framework of the four-particle cluster approximation for the proton ordering model, the thermodynamic and longitudinal dielectric, piezoelectric, and elastic characteristics of the KD_2PO_4 have been calculated. It was shown that at the proper choice of the model parameters a good quantitative description of available experimental data by the proposed theory is obtained.

In this work, following the approach developed in [37], we shall calculate the longitudinal dynamic dielectric characteristics of the KD_2PO_4 type ferroelectrics and study their temperature and frequency dependences. We shall investigate the effect of crystal clamping by longitudinal high-frequency external electric field. Expressions for the sound velocity and attenuation for a certain propagation direction will be obtained; their temperature and frequency dependences will be explored.

2. System of equations for time-dependent distribution functions of deuterons

We shall consider a system of deuterons moving on O–D. . . O bonds in deuterated ferroelectric of the KD_2PO_4 type. A primitive Bravais cell of these crystals consists of two PO_4 groups (tetrahedra) with four hydrogen bonds attached to one of them ("A" type tetrahedra), while the hydrogen bond attached to the other tetrahedron ("B" type) belongs to the four nearest structure elements surrounding it (figure 1).

The Hamiltonian of the deuteron subsystem with taking into account short-range and long-range interactions in the presence of mechanical stress $\sigma_6 = \sigma_{xy}$ and electric field E_3 along the

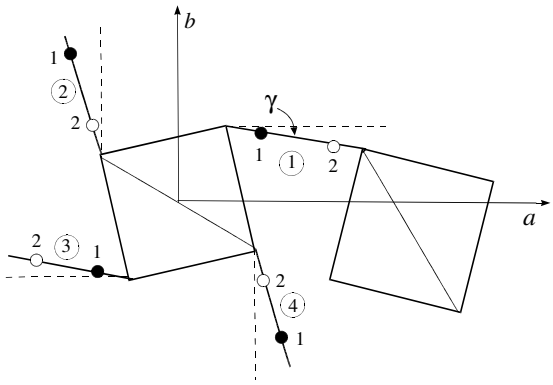

Figure 1. Primitive Bravais cell of the KD_2PO_4 type crystal. One of the possible ferroelectric configurations is shown.

crystallographic axis c, which induce contributions to polarization P_3 and strain ε_6 of the crystal, consists of the "seed" and pseudospin parts [33,35]:

$$\hat{H} = NH^{(0)} + \hat{H}_s\,, \tag{2.1}$$

where N is the number of primitive cells. The "seed" energy of the primitive cell corresponds to the heavy ion subsystem and does not depend explicitly on hydrogen arrangement. It is expressed via the strain ε_6 and electric field E_3 and includes the elastic, piezoelectric, and electric counterparts

$$H^{(0)} = \bar{v}\left(\frac{1}{2}c_{66}^{E0}\varepsilon_6^2 - e_{36}^0 E_3\varepsilon_6 - \frac{1}{2}\chi_{33}^{\varepsilon 0}E_3^2\right), \tag{2.2}$$

where $\bar{v} = \frac{v}{k_{\rm B}}$, v is the primitive cell volume; c_{66}^{E0}, e_{36}^0, $\chi_{33}^{\varepsilon 0}$ are the so-called "seed" elastic constant, coefficient of the piezoelectric stress, and dielectric susceptibility, respectively. These quantities determine the temperature behavior of the corresponding observable characteristics far from the transition point $T_{\rm c}$.

The pseudospin part of the Hamiltonian is

$$\hat{H} = N\left[H^0 + 2\nu_{\rm c}(\eta^{(1)})^2\right] + \sum_q \hat{H}_{q6}^{(4)},$$

where

$$\begin{aligned}\hat{H}_{q6}^{(4)} \;=\; & -\sum_{f=1}^{4}\frac{z_6}{\beta}\frac{\sigma_{qf}}{2} + \frac{\varepsilon_6}{4}(-\delta_{s6}+2\delta_{16})\sum_{f=1}^{4}\frac{\sigma_{qf}}{2} \\ & - \varepsilon_6(\delta_{s6}+2\delta_{16})\Big(\frac{\sigma_{q1}}{2}\frac{\sigma_{q2}}{2}\frac{\sigma_{q3}}{2}+\frac{\sigma_{q1}}{2}\frac{\sigma_{q2}}{2}\frac{\sigma_{q4}}{2}+\frac{\sigma_{q1}}{2}\frac{\sigma_{q3}}{2}\frac{\sigma_{q4}}{2}+\frac{\sigma_{q2}}{2}\frac{\sigma_{q3}}{2}\frac{\sigma_{q4}}{2}\Big) \\ & + (V+\delta_{a6}\varepsilon_6)\left(\frac{\sigma_{q1}}{2}\frac{\sigma_{q2}}{2}+\frac{\sigma_{q3}}{2}\frac{\sigma_{q4}}{2}\right)+(V-\delta_{a6}\varepsilon_6)\left(\frac{\sigma_{q2}}{2}\frac{\sigma_{q3}}{2}+\frac{\sigma_{q4}}{2}\frac{\sigma_{q1}}{2}\right) \\ & + U\left(\frac{\sigma_{q1}}{2}\frac{\sigma_{q3}}{2}+\frac{\sigma_{q2}}{2}\frac{\sigma_{q4}}{2}\right)+\Phi\frac{\sigma_{q1}}{2}\frac{\sigma_{q2}}{2}\frac{\sigma_{q3}}{2}\frac{\sigma_{q4}}{2},\end{aligned} \tag{2.3}$$

and

$$z_6 = \beta(-\Delta^c + 2\nu_{\rm c}\eta^{(1)} - 2\psi_6\varepsilon_6 + \mu_3 E_3), \qquad \left(\beta = \frac{1}{k_{\rm B}T}\right).$$

The dynamic properties of the KD_2PO_4 type ferroelectrics will be explored within the proposed dynamic model [21], based on the stochastic Glauber model [16] ideas. When calculating the

dynamic characteristics, we shall restrict our consideration to the four-particle cluster approximation, providing a successful description of thermodynamic characteristics of the crystals [8–10,15]. Using the approach, developed in [18–21], we obtain the following system of equations for the time-dependent deuteron distribution functions:

$$-\alpha\frac{\mathrm{d}}{\mathrm{d}t}\left\langle\prod_f\sigma_{qf}\right\rangle=\sum_{f'}\left\{\left\langle\prod_f\sigma_{qf}\left[1-\sigma_{qf'}\tanh\frac{1}{2}\beta\varepsilon^z_{qf'}(t)\right]\right\rangle\right\}, \tag{2.4}$$

where $\varepsilon^z_{qf'}(t)$ is the local field acting on the f'th deuteron in the qth cell, which can be found from the Hamiltonian (2.3).

The expressions $\tanh\frac{\beta\varepsilon^z_{qf'}(t)}{2}$ are presented in the following form

$$\begin{aligned}
\tanh\frac{\beta\varepsilon^z_{q1}}{2}&=P^z_6\sigma_{q3}+Q^z_{61}\sigma_{q2}+Q^z_{62}\sigma_{q4}+R^z_6\sigma_{q2}\sigma_{q3}\sigma_{q4}\\
&\quad+M^z_{61}\sigma_{q2}\sigma_{q3}+M^z_{62}\sigma_{q3}\sigma_{q4}+N^z_6\sigma_{q2}\sigma_{q4}+L^z_6\,,\\
\tanh\frac{\beta\varepsilon^z_{q2}}{2}&=P^z_6\sigma_{q4}+Q^z_{61}\sigma_{q1}+Q^z_{62}\sigma_{q3}+R^z_6\sigma_{q1}\sigma_{q3}\sigma_{q4}\\
&\quad+M^z_{61}\sigma_{q4}\sigma_{q2}+M^z_{62}\sigma_{q3}\sigma_{q4}+N^z_6\sigma_{q1}\sigma_{q3}+L^z_6\,,\\
\tanh\frac{\beta\varepsilon^z_{q3}}{2}&=P^z_6\sigma_{q1}+Q^z_{61}\sigma_{q4}+Q^z_{62}\sigma_{q2}+R^z_6\sigma_{q1}\sigma_{q2}\sigma_{q4}\\
&\quad+M^z_{61}\sigma_{q1}\sigma_{q4}+M^z_{62}\sigma_{q1}\sigma_{q2}+N^z_6\sigma_{q2}\sigma_{q4}+L^z_6\,,\\
\tanh\frac{\beta\varepsilon^z_{q4}}{2}&=P^z_6\sigma_{q2}+Q^z_{61}\sigma_{q3}+Q^z_{62}\sigma_{q1}+R^z_6\sigma_{q1}\sigma_{q2}\sigma_{q3}\\
&\quad+M^z_{61}\sigma_{q2}\sigma_{q3}+M^z_{62}\sigma_{q1}\sigma_{q2}+N^z_6\sigma_{q1}\sigma_{q2}+L^z_6\,.
\end{aligned}\tag{2.5}$$

Since $\sigma_{qf}=\pm1$, we find for the coefficients $P_6,\ldots,L_6$:

$$\begin{aligned}
P^z_6&=\frac{1}{8}(l^z_1-l^z_2+n^z_1-n^z_2+m^z_1-m^z_2+m^z_3-m^z_4),\\
Q^z_{61}&=\frac{1}{8}(l^z_1-l^z_2-n^z_1+n^z_2+m^z_1+m^z_2-m^z_3-m^z_4),\\
Q^z_{62}&=\frac{1}{8}(l^z_1-l^z_2-n^z_1+n^z_2-m^z_1-m^z_2+m^z_3+m^z_4),\\
R^z_6&=\frac{1}{8}(l^z_1-l^z_2+n^z_1-n^z_2-m^z_1+m^z_2-m^z_3+m^z_4),\\
N^z_6&=\frac{1}{8}(l^z_1+l^z_2+n^z_1+n^z_2-m^z_1-m^z_2-m^z_3-m^z_4),\\
M^z_{61}&=\frac{1}{8}(l^z_1+l^z_2-n^z_1-n^z_2+m^z_1-m^z_2-m^z_3+m^z_4),\\
M^z_{62}&=\frac{1}{8}(l^z_1+l^z_2-n^z_1-n^z_2-m^z_1+m^z_2+m^z_3-m^z_4),\\
L^z_6&=\frac{1}{8}(l^z_1+l^z_2+n^z_1+n^z_2+m^z_1+m^z_2+m^z_3+m^z_4),
\end{aligned}\tag{2.6}$$

where we use the following notations

$$\begin{aligned}
l^z_{\frac{1}{2}}&=\tanh\frac{\beta}{2}\left[\pm w+(\delta_{s6}+\delta_{16})\varepsilon_6+\frac{z^z_6}{\beta}\right],\qquad n^z_{\frac{1}{2}}=\tanh\frac{\beta}{2}\left[\pm(w-w_1)-\delta_{16}\varepsilon_6+\frac{z^z_6}{\beta}\right],\\
m^z_{\frac{1}{4}}&=\tanh\frac{\beta}{2}\left[\pm(\varepsilon-\delta_{a6}\varepsilon_6-w)-\delta_{16}\varepsilon_6+\frac{z^z_6}{\beta}\right],\quad m^z_{\frac{2}{3}}=\tanh\frac{\beta}{2}\left[\mp(\varepsilon+\delta_{a6}\varepsilon_6-w)-\delta_{16}\varepsilon_6+\frac{z^z_6}{\beta}\right].
\end{aligned}$$

Taking into account the symmetry of distribution functions

$$\begin{aligned}
\eta^{(1)z}&=\langle\sigma_{q1}\rangle=\langle\sigma_{q2}\rangle=\langle\sigma_{q3}\rangle=\langle\sigma_{q4}\rangle,\\
\eta^{(3)z}&=\langle\sigma_{q1}\sigma_{q2}\sigma_{q3}\rangle=\langle\sigma_{q1}\sigma_{q3}\sigma_{q4}\rangle=\langle\sigma_{q1}\sigma_{q2}\sigma_{q4}\rangle=\langle\sigma_{q2}\sigma_{q3}\sigma_{q4}\rangle,\\
\eta^{(2)z}_1&=\langle\sigma_{q2}\sigma_{q3}\rangle=\langle\sigma_{q1}\sigma_{q4}\rangle,\quad \eta^{(2)z}_2=\langle\sigma_{q1}\sigma_{q2}\rangle=\langle\sigma_{q3}\sigma_{q4}\rangle,\quad \eta^{(2)z}_3=\langle\sigma_{q1}\sigma_{q3}\rangle=\langle\sigma_{q2}\sigma_{q4}\rangle,
\end{aligned}\tag{2.7}$$

from (2.4) with taking into account (2.5) and (2.7), we can obtain a closed system of equations for the time-dependent single-particle, pair, and three-particle deuteron distribution functions in the KD_2PO_4 type crystals

$$\alpha\frac{\mathrm{d}}{\mathrm{d}t}\begin{pmatrix}\eta^{(1)z}\\ \eta^{(3)z}\\ \eta_1^{(2)z}\\ \eta_2^{(2)z}\\ \eta_3^{(2)z}\end{pmatrix}=\begin{pmatrix}\bar{c}_{11}&\bar{c}_{12}&\bar{c}_{13}&\bar{c}_{14}&\bar{c}_{15}\\ \bar{c}_{21}&\bar{c}_{22}&\bar{c}_{23}&\bar{c}_{24}&\bar{c}_{25}\\ \bar{c}_{31}&\bar{c}_{32}&\bar{c}_{33}&\bar{c}_{34}&\bar{c}_{35}\\ \bar{c}_{41}&\bar{c}_{42}&\bar{c}_{43}&\bar{c}_{44}&\bar{c}_{45}\\ \bar{c}_{51}&\bar{c}_{52}&\bar{c}_{53}&\bar{c}_{54}&\bar{c}_{55}\end{pmatrix}\begin{pmatrix}\eta^{(1)z}\\ \eta^{(3)z}\\ \eta_1^{(2)z}\\ \eta_2^{(2)z}\\ \eta_3^{(2)z}\end{pmatrix}+\begin{pmatrix}\bar{c}_1\\ \bar{c}_2\\ \bar{c}_3\\ \bar{c}_4\\ \bar{c}_5\end{pmatrix}. \tag{2.8}$$

Here we use the following notations

$$\begin{aligned}
\bar{c}_{11} &= -(1-P_6^z-Q_{61}^z-Q_{62}^z),\ \bar{c}_{12}=R_6^z,\ \bar{c}_{13}=M_{61}^z,\ \bar{c}_{14}=M_{62}^z,\ \bar{c}_{15}=N_6^z,\ \bar{c}_1=L_6^z,\\
\bar{c}_{21} &= (2P_6^z+2Q_{61}^z+2Q_{62}^z+3R_6),\ \bar{c}_{22}=-(3-P_6^z-Q_{61}^z-Q_{62}^z),\ \bar{c}_{23}=(N_6^z+M_{62}^z+L_6^z),\\
\bar{c}_{24} &= (N_6^z+M_{61}^z+L_6^z),\ \bar{c}_{25}=(M_{61}^z+M_{62}^z+L_6^z),\ \bar{c}_2=(N_6^z+M_{61}^z+M_{62}^z),\\
\bar{c}_{31} &= 2(N_6^z+M_{62}^z+L_6^z),\ \bar{c}_{32}=2M_{61}^z,\ \bar{c}_{33}=-2(1-R_6^z),\ \bar{c}_{34}=2P_6^z,\ \bar{c}_{35}=2Q_{61}^z,\ \bar{c}_3=2Q_{62}^z,\\
\bar{c}_{41} &= 2(N_6^z+M_{61}^z+L_6^z),\ \bar{c}_{42}=2M_{62}^z,\ \bar{c}_{43}=2P_6^z,\ \bar{c}_{44}=-2(1-R_6^z),\ \bar{c}_{45}=2Q_{62}^z,\ \bar{c}_4=2Q_{61}^z,\\
\bar{c}_{51} &= 2(M_{61}^z+M_{62}^z+L_6^z),\ \bar{c}_{52}=2N_6^z,\ \bar{c}_{53}=2Q_{61}^z,\ \bar{c}_{54}=2Q_{62}^z,\ \bar{c}_{55}=-2(1-R_6^z),\ \bar{c}_5=2P_6^z.
\end{aligned} \tag{2.9}$$

In the single-particle approximation from (2.4) we obtain the following equation for distribution functions

$$\alpha\frac{\mathrm{d}}{\mathrm{d}t}\eta^{(1)z}=-\eta^{(1)z}+\tanh\frac{1}{2}\bar{z}_6^z. \tag{2.10}$$

3. Dynamic characteristics of a mechanically free $K(H_{1-x}D_x)_2PO_4$ crystal. Piezoelectric resonance

In this section we shall consider vibrations of a thin $l\times l$ square plate of a KD_2PO_4 crystal, cut in the [001] plane, induced by time-dependent electric field $E_{3t}=E_3\mathrm{e}^{\mathrm{i}\omega t}$. This field, in addition to the shear strain ε_6, also induces diagonal components of the strain tensor ε_i. For the sake of simplicity, we shall neglect the diagonal strains.

Dynamics of deformational processes in KD_2PO_4 will be described using classical Newtonian equations of motion of an elementary volume

$$\rho\frac{\partial^2u_i}{\partial t^2}=\sum_k\frac{\partial\sigma_{ik}}{\partial x_k}, \tag{3.1}$$

where ρ is the cell volume, u_i are the displacements of an elementary volume along the axis x_i, σ_{ik} is the mechanical stress. The shear strain ε_6 is determined by the displacements $u_x=u_1$ and $u_y=u_z$, that is

$$\varepsilon_6=\varepsilon_{xy}=\frac{\partial u_1}{\partial y}+\frac{\partial u_2}{\partial x}.$$

In our case a shear strain $\sigma_{xy}=\sigma_6$ is different from zero and [36]

$$\sigma_6=c_{66}^{E0}\varepsilon_6-e_{36}^0E_3+\frac{4\psi_6}{v}\frac{m^z}{D_6^z}+\frac{2\delta_{a6}}{\bar{v}D_6^z}M_{a6}-\frac{2\delta_{s6}}{vD_6^z}M_{s6}+\frac{2\delta_{16}}{vD_6^z}M_{16}, \tag{3.2}$$

where

$$M_{a6}=aa_6-\frac{a}{a_6},\qquad M_{s6}=\sinh(2z_6^z+\beta\delta_{s6}\varepsilon_6),\qquad M_{16}=4b\sinh(z_6^z-\beta\delta_{16}\varepsilon_6).$$

Thus,

$$\rho\frac{\partial^2 u_1}{\partial t^2} = c_{66}^{E0}\frac{\partial\varepsilon_6}{\partial y} + \frac{4\psi_6}{v}\frac{\partial\eta^{(1)}}{\partial y} + \frac{2\delta_{a6}}{v}\frac{\partial}{\partial y}\left(\frac{M_{a6}}{D_6}\right) - \frac{2\delta_{s6}}{v}\frac{\partial}{\partial y}\left(\frac{M_{s6}}{D_6}\right) + \frac{2\delta_{16}}{v}\frac{\partial}{\partial y}\left(\frac{M_{16}}{D_6}\right), \quad (3.3)$$
$$\rho\frac{\partial^2 u_2}{\partial t^2} = c_{66}^{E0}\frac{\partial\varepsilon_6}{\partial x} + \frac{4\psi_6}{v}\frac{\partial\eta^{(1)}}{\partial x} + \frac{2\delta_{a6}}{v}\frac{\partial}{\partial x}\left(\frac{M_{a6}}{D_6}\right) - \frac{2\delta_{s6}}{v}\frac{\partial}{\partial x}\left(\frac{M_{s6}}{D_6}\right) + \frac{2\delta_{16}}{v}\frac{\partial}{\partial x}\left(\frac{M_{16}}{D_6}\right).$$

At small deviations from the equilibrium we can separate in the systems (2.6) and (2.8) the static and time-dependent parts, presenting the distribution functions, effective displacement fields u_1, u_2, and the strain ε_6 as sums of equilibrium values and of fluctuational deviations

$$\begin{aligned}
&\eta^{(1)} = \tilde\eta^{(1)} + \eta_t^{(1)}, \qquad \eta^{(3)} = \tilde\eta^{(3)} + \eta_t^{(3)}, \qquad \eta_i^{(2)} = \tilde\eta_i^{(2)} + \eta_t^{(2)}, \qquad (i=1,2,3),\\
&\varepsilon_6 = \tilde\varepsilon_6 + \varepsilon_{6t}, \qquad u_{1,2} = \tilde u_{1,2} + u_{1,2t},\\
&z_6^z = \tilde z_6 + z_{6t} = -\beta\tilde\Delta + 2\beta\nu_c\tilde\eta^{(1)} - 2\beta\psi_6\varepsilon_6 - \beta\Delta_t + 2\beta\nu_c\eta_t^{(1)} - 2\beta\psi_6\varepsilon_{6t} + \beta\mu_3 E_{3t}\,.
\end{aligned} \quad (3.4)$$

We substitute the expressions (3.4) into the system of equations (2.8), (2.10), expand into a series over the time dependent terms the coefficients $\bar c_{ij}$, $\bar c_i$, limit oneself to linear approximation. We exclude parameter Δ_t and obtain the system of equations for fluctuating parts of distribution functions:

$$\begin{aligned}
\frac{\mathrm{d}}{\mathrm{d}t}\begin{pmatrix}\eta_t^{(1)}\\ \eta_t^{(3)}\\ \eta_{1t}^{(2)}\\ \eta_{2t}^{(2)}\\ \eta_{3t}^{(2)}\end{pmatrix} &= \begin{pmatrix} c_{11} & c_{12} & c_{13} & c_{14} & c_{15}\\ c_{21} & c_{22} & c_{23} & c_{24} & c_{25}\\ c_{31} & c_{32} & c_{33} & c_{34} & c_{35}\\ c_{41} & c_{42} & c_{43} & c_{44} & c_{45}\\ c_{51} & c_{52} & c_{53} & c_{54} & c_{55}\end{pmatrix}\begin{pmatrix}\eta_t^{(1)}\\ \eta_t^{(3)}\\ \eta_{1t}^{(2)}\\ \eta_{2t}^{(2)}\\ \eta_{3t}^{(2)}\end{pmatrix} - \frac{1}{2}\beta\mu_3 E_{3t}\begin{pmatrix}c_1\\ c_2\\ c_3\\ c_4\\ c_5\end{pmatrix}\\
&+\beta\psi_6\varepsilon_{6t}\begin{pmatrix}c_1\\ c_2\\ c_3\\ c_4\\ c_5\end{pmatrix} - \beta\delta_{s6}\varepsilon_{6t}\begin{pmatrix}c_{1s}\\ c_{3s}\\ c_{21s}\\ c_{22s}\\ c_{23s}\end{pmatrix} + \beta\delta_{a6}\varepsilon_{6t}\begin{pmatrix}c_{1a}\\ c_{3a}\\ c_{21a}\\ c_{22a}\\ c_{23a}\end{pmatrix} - \beta\delta_{16}\varepsilon_{6t}\begin{pmatrix}\tilde c_{11}\\ \tilde c_{21}\\ \tilde c_{31}\\ \tilde c_{41}\\ \tilde c_{51}\end{pmatrix}.
\end{aligned} \quad (3.5)$$

The expressions for coefficients of the system (3.5) are given in [36].

Taking into account (3.4), equations for the displacements (3.3) can be rewritten as follows:

$$\rho\frac{\partial^2 u_{1t}}{\partial t^2} = c_{16}\frac{\partial\varepsilon_{6t}}{\partial y} + c_{26}\frac{\partial\eta_t^{(1)}}{\partial y}\,, \qquad \rho\frac{\partial^2 u_{2t}}{\partial t^2} = c_{16}\frac{\partial\varepsilon_{6t}}{\partial x} + c_{26}\frac{\partial\eta_t^{(1)}}{\partial x}\,, \quad (3.6)$$

where we use the following notations

$$\begin{aligned}
c_{16} &= c_{66}^{E0} + \frac{4\beta\psi_6}{vD_6}f_6 - \frac{2\beta}{vD_6}\Big[\delta_{s6}^2\cosh(2\tilde z_6 + \beta\delta_{s6}\tilde\varepsilon_6) + \delta_{16}^2 4b\cosh(\tilde z_6 - \beta\delta_{16}\tilde\varepsilon_6)\\
&\quad +\delta_{a6}^2 2a\cosh\beta\delta_{a6}\tilde\varepsilon_6\Big] + \frac{2\beta}{vD_6^2}(-\delta_{s6}M_{s6} + \delta_{16}M_{16} + \delta_{a6}M_{a6})^2,\\
c_{26} &= \frac{4}{v}\left(\psi_6 - \frac{\varphi_6^\eta}{D_6}f_6\right),
\end{aligned}$$

We shall look for solutions of the system (3.5) and (3.6) in the form of harmonic waves

$$\begin{aligned}
&\eta_t^{(1)} = \eta^{(1)}(6,x,y)\mathrm{e}^{\mathrm{i}\omega t}, \qquad \eta_t^{(3)} = \eta^{(3)}(6,x,y)\mathrm{e}^{\mathrm{i}\omega t},\\
&\eta_{1t}^{(2)} = \eta_1^{(2)}(6,x,y)\mathrm{e}^{\mathrm{i}\omega t}, \qquad \eta_{2t}^{(2)} = \eta_2^{(2)}(6,x,y)\mathrm{e}^{\mathrm{i}\omega t},\\
&\eta_{3t}^{(2)} = \eta_3^{(2)}(6,x,y)\mathrm{e}^{\mathrm{i}\omega t}, \qquad \varepsilon_{6t} = \varepsilon_6(x,y)\mathrm{e}^{\mathrm{i}\omega t},\\
&u_{1t} = u_1(y)\mathrm{e}^{\mathrm{i}\omega t}, \qquad u_{2t} = u_2(x)\mathrm{e}^{\mathrm{i}\omega t}.
\end{aligned} \quad (3.7)$$

Finally, solving the system (3.5) with taking into account (3.7), we find that

$$\begin{aligned}\eta^{(1)}(6,x,y) &= \frac{\beta\mu_3}{2}F^{(1)}(\alpha\omega)E_3+\Big[-\beta\psi_6F^{(1)}(\alpha\omega)\\ &\quad+\beta\delta_{s6}F_s^{(1)}(\alpha\omega)-\beta\delta_{a6}F_a^{(1)}(\alpha\omega)+\beta\delta_{16}F_1^{(1)}(\alpha\omega)\Big]\varepsilon_6(x,y),\end{aligned}\tag{3.8}$$

where we use the notations

$$\begin{aligned}F^{(1)}(\alpha\omega)&=\frac{p^{(4)}(\mathrm{i}\alpha\omega)^4+p^{(3)}(\mathrm{i}\alpha\omega)^3+p^{(2)}(\mathrm{i}\alpha\omega)^2+p^{(1)}(\mathrm{i}\alpha\omega)+p^{(0)}}{(\mathrm{i}\alpha\omega)^5+p_4(\mathrm{i}\alpha\omega)^4+p_3(\mathrm{i}\alpha\omega)^3+p_2(\mathrm{i}\alpha\omega)^2+p_1(\mathrm{i}\alpha\omega)+p_0},\\ F_s^{(1)}(\alpha\omega)&=\frac{p_s^{(4)}(\mathrm{i}\alpha\omega)^4+p_s^{(3)}(\mathrm{i}\alpha\omega)^3+p_s^{(2)}(\mathrm{i}\alpha\omega)^2+p_s^{(1)}(\mathrm{i}\alpha\omega)+p_s^{(0)}}{(\mathrm{i}\alpha\omega)^5+p_4(\mathrm{i}\alpha\omega)^4+p_3(\mathrm{i}\alpha\omega)^3+p_2(\mathrm{i}\alpha\omega)^2+p_1(\mathrm{i}\alpha\omega)+p_0},\\ F_a^{(1)}(\alpha\omega)&=\frac{p_a^{(4)}(\mathrm{i}\alpha\omega)^4+p_a^{(3)}(\mathrm{i}\alpha\omega)^3+p_a^{(2)}(\mathrm{i}\alpha\omega)^2+p_a^{(1)}(\mathrm{i}\alpha\omega)+p_a^{(0)}}{(\mathrm{i}\alpha\omega)^5+p_4(\mathrm{i}\alpha\omega)^4+p_3(\mathrm{i}\alpha\omega)^3+p_2(\mathrm{i}\alpha\omega)^2+p_1(\mathrm{i}\alpha\omega)+p_0},\\ F_1^{(1)}(\alpha\omega)&=\frac{p_1^{(4)}(\mathrm{i}\alpha\omega)^4+p_1^{(3)}(\mathrm{i}\alpha\omega)^3+p_1^{(2)}(\mathrm{i}\alpha\omega)^2+p_1^{(1)}(\mathrm{i}\alpha\omega)+p_1^{(0)}}{(\mathrm{i}\alpha\omega)^5+p_4(\mathrm{i}\alpha\omega)^4+p_3(\mathrm{i}\alpha\omega)^3+p_2(\mathrm{i}\alpha\omega)^2+p_1(\mathrm{i}\alpha\omega)+p_0}.\end{aligned}\tag{3.9}$$

Expressions for $p_4,\dots,p_0$, $p^{(4)},\dots,p^{(0)}$, $p_s^{(4)},\dots,p_s^{(0)}$, $p_a^{(4)},\dots,p_a^{(0)}$, $p_1^{(4)},\dots,p_1^{(0)}$ in (3.9) are given in [36].

Taking into account the relations (3.6) and (3.7), we obtain the following wave equations for u_1, u_2:

$$c_{66}^E(\alpha\omega)\frac{\partial^2u_1}{\partial y^2}+\rho\omega^2u_1=0,\qquad c_{66}^E(\alpha\omega)\frac{\partial^2u_2}{\partial x^2}+\rho\omega^2u_2=0,\tag{3.10}$$

where

$$\begin{aligned}c_{66}^E(\alpha\omega) &= c_{66}^{E0}+\frac{4\beta\psi_6}{vD_6}f_6+\frac{2\beta}{vD_6^2}(-\delta_{s6}M_{s6}+\delta_{16}M_{16}+\delta_{a6}M_{a6})^2\\ &\quad+\frac{4\beta\psi_6}{v}\Big[-\psi_6F^{(1)}(\alpha\omega)+\delta_{s6}F_s^{(1)}(\alpha\omega)+\delta_{16}F_1^{(1)}(\alpha\omega)-\delta_{a6}F_a^{(1)}(\alpha\omega)\Big]\\ &\quad-\frac{4\varphi_3f_6}{vD_6}\beta\Big[-\psi_6F^{(1)}(\alpha\omega)+\delta_{s6}F_s^{(1)}(\alpha\omega)+\delta_{16}F_1^{(1)}(\alpha\omega)-\delta_{a6}F_a^{(1)}(\alpha\omega)\Big]\\ &\quad-\frac{2\beta}{vD_6}\Big[\delta_{s6}^2\cosh(2\tilde z+\beta\delta_{s6}\tilde\varepsilon_6)+4b\delta_{16}^2\cosh(\tilde z-\beta\delta_{16}\tilde\varepsilon_6)+\delta_{a6}^2 2a\cosh\beta\delta_{a6}\tilde\varepsilon_6^2\Big].\end{aligned}$$

Equation (3.10) can be written as

$$\frac{\partial^2u_1}{\partial y^2}+k_6^2u_1=0,\qquad \frac{\partial^2u_2}{\partial x^2}+k_6^2u_2=0,\tag{3.11}$$

where k_6 is the wavenumber

$$k_6=\frac{\omega\sqrt{\rho}}{\sqrt{c_{66}^E(\alpha\omega)}}.\tag{3.12}$$

We shall look for the solutions of (3.11) in the form

$$u_1=A_1\cos k_6y+B_1\sin k_6y,\qquad u_2=A_2\cos k_6x+B_2\sin k_6x.$$

As a result

$$\varepsilon_6(x,y)=k_6\Big[-(A_1\cos k_6y+A_2\cos k_6x)+(B_1\sin k_6y+B_2\sin k_6x)\Big].\tag{3.13}$$

The boundary conditions are set as follows:

$$\varepsilon_6(0,0)=\varepsilon_6(l,l)=\varepsilon_6(0,l)=\varepsilon_6(l,0)=\varepsilon_0.\tag{3.14}$$

The values of ε_0 are determined from (3.2), using the relation (3.10)

$$\varepsilon_0 = \frac{e_{36}(\alpha\omega)}{c_{66}^E(\alpha\omega)} E_3 \,. \tag{3.15}$$

where

$$e_{36}(\alpha\omega) = e_{36}^0 + \frac{\beta\mu_3}{v}\Big[-\psi_6 F^{(1)}(\alpha\omega) + \delta_{s6}F_s^{(1)}(\alpha\omega) + \delta_{16}F_1^{(1)}(\alpha\omega) - \delta_{a6}F_a^{(1)}(\alpha\omega)\Big]. \tag{3.16}$$

Taking into account the boundary conditions (3.14), we find from (3.13)

$$\varepsilon_6(x,y) = \frac{\varepsilon_0}{2}\left[-\frac{\cos k_6 l - 1}{\sin k_6 l}(\sin k_6 y + \sin k_6 x) + (\cos k_6 y + \cos k_6 x)\right]. \tag{3.17}$$

Using the expression, relating polarization P_3 to the order parameter $\eta^{(1)}$ and strain ε_6, as well as relation (3.8), we find that

$$P_3(x,y,t) = P_3(x,y)\mathrm{e}^{\mathrm{i}\omega t}, \tag{3.18}$$

where

$$P_3(x,y) = e_{36}(\alpha\omega)\varepsilon_6(x,y) + \chi_{33}^{\varepsilon}(\alpha\omega)E_3 \,,$$

and

$$\chi_{33}(\alpha\omega) = \chi_{33}^{\varepsilon 0} + \frac{\beta\mu_3^2}{2v}F^{(1)}(\alpha\omega).$$

Now we can calculate the dynamic dielectric susceptibility of a free crystal $\chi_{33}^{\sigma}(\alpha\omega)$

$$\chi_{33}^{\sigma}(\alpha\omega) = \frac{1}{l^2}\frac{\partial}{\partial E_3}\int_0^l\int_0^l P_3(x,y)\mathrm{d}x\mathrm{d}y. \tag{3.19}$$

Taking into account (3.17), we find that

$$\frac{1}{l^2}\int_0^l\int_0^l \mathrm{d}x\mathrm{d}y\varepsilon_6(x,y) = \frac{2\varepsilon_0}{k_6}\tan\frac{k_6 l}{2} = \frac{\varepsilon_0}{R(\omega)} \,, \tag{3.20}$$

where

$$\frac{1}{R(\omega)} = \frac{2}{k_6 l}\tan\frac{k_6 l}{2} \,.$$

With (3.18) and (3.20) from (3.19) we obtain that

$$\chi_{33}^{\sigma}(\alpha\omega) = \chi_{33}^{\varepsilon}(\alpha\omega) + \frac{1}{R(\omega)}\frac{e_{36}^2(\alpha\omega)}{c_{66}^E(\alpha\omega)} \,. \tag{3.21}$$

4. Attenuation and velocity of ultrasound in KD_2PO_4 crystals

Pulsed ultrasonics provide a useful method for the investigation of crystal behavior. The ultrasound wavelength is usually much smaller than the sample dimensions. Therefore, the dynamical variables, such as elementary displacements and order parameter, depend only on the spatial coordinate which is the direction of sound propagation.

If thin bars of the crystal are cut along [001], then we shall consider a transverse sound wave propagating along the bar and polarized along [010]. Among $\frac{\partial u_i}{\partial x_j}$ the only nonzero derivative is

$\frac{\partial u_2}{\partial x}$; therefore, instead of the systems (3.5) and (3.6), we can write

$$\frac{\mathrm{d}}{\mathrm{d}t}\begin{pmatrix}\eta_t^{(1)}\\ \eta_t^{(3)}\\ \eta_{1t}^{(2)}\\ \eta_{2t}^{(2)}\\ \eta_{3t}^{(2)}\end{pmatrix} = \begin{pmatrix} c_{11} & c_{12} & c_{13} & c_{14} & c_{15}\\ c_{21} & c_{22} & c_{23} & c_{24} & c_{25}\\ c_{31} & c_{32} & c_{33} & c_{34} & c_{35}\\ c_{41} & c_{42} & c_{43} & c_{44} & c_{45}\\ c_{51} & c_{52} & c_{53} & c_{54} & c_{55}\end{pmatrix}\begin{pmatrix}\eta_t^{(1)}\\ \eta_t^{(3)}\\ \eta_{1t}^{(2)}\\ \eta_{2t}^{(2)}\\ \eta_{3t}^{(2)}\end{pmatrix}$$

$$+\beta\psi_6\varepsilon_{6t}\begin{pmatrix}c_1\\ c_2\\ c_3\\ c_4\\ c_5\end{pmatrix} - \beta\delta_{s6}\varepsilon_{6t}\begin{pmatrix}c_{1s}\\ c_{3s}\\ c_{21s}\\ c_{22s}\\ c_{23s}\end{pmatrix} + \beta\delta_{a6}\varepsilon_{6t}\begin{pmatrix}c_{1a}\\ c_{3a}\\ c_{21a}\\ c_{22a}\\ c_{23a}\end{pmatrix} - \beta\delta_{16}\varepsilon_{6t}\begin{pmatrix}\tilde{c}_{11}\\ \tilde{c}_{21}\\ \tilde{c}_{31}\\ \tilde{c}_{41}\\ \tilde{c}_{51}\end{pmatrix},$$

$$\rho\frac{\partial^2 u_{2t}}{\partial t^2} = c_{16}\frac{\partial\varepsilon_{6t}}{\partial x} + c_{26}\frac{\partial\eta_t^{(1)}}{\partial x}. \tag{4.1}$$

Solving the system (4.1), we obtain the same wavenumber as found above

$$k_6 = \frac{\omega\sqrt{\rho}}{\sqrt{c_{66}^E(\alpha\omega)}}. \tag{4.2}$$

Using (4.2), we can find the sound wave velocity

$$v_{66}(\omega) = \frac{\omega}{\mathrm{Re}|k_6|} = \mathrm{Re}\frac{\sqrt{c_{66}^E(\alpha\omega)}}{\sqrt{\rho}} \tag{4.3}$$

and the contribution of the pseudospin subsystem to the sound attenuation

$$\alpha_6(\omega) = \alpha_{60} - \mathrm{Im}|k_6| = \alpha_{60} - \mathrm{Im}\left|\frac{\omega\sqrt{\rho}}{\sqrt{c_{66}^E(\alpha\omega)}}\right|, \tag{4.4}$$

where α_{60} is a constant frequency and temperature independent contribution of the other mechanisms to the experimentally observable attenuation.

5. Discussion

Let us evaluate the above found dynamic characteristics of mechanically free $K(H_{1-x}D_x)_2PO_4$ crystals, cut as $l \times l$ square plates ($l = 1$ mm) in the [0,0,1] plane. It should be noted that the developed theory is valid, strictly speaking, for highly deuterated KD_2PO_4 crystals, only. However, the tunneling in undeuterated crystals is weakened due to short-range interactions [26], which is indicated by the experimentally established relaxational character of $\varepsilon_{33}^*(\nu, T)$ dispersion see [15,23–25] in KH_2PO_4. Therefore, proton tunneling can be neglected as well as the obtained expressions used for undeuterated KH_2PO_4. In numerical calculations we shall use the values of the model parameters determined in describing the static and dynamic permittivity of a mechanical free crystal [36] and given in table 1.

Unfortunately, no experimental data are available to perform a quantitative comparison of the theoretically obtained temperature and frequency dependences of the dynamic characteristics of mechanically free crystals in the piezoelectric resonance region.

In figures 2 and 3 we plot the frequency dependences of the real and imaginary parts of the dynamic dielectric permittivity of mechanically free KH_2PO_4, KD_2PO_4 crystals in the paraelectric phase at different temperatures ΔT. For the MH_2XO_4 crystals, a resonance dispersion takes place in the frequency range, $3 \cdot 10^5$–$3 \cdot 10^8$ Hz, and for KD_2PO_4 in the $5 \cdot 10^5$–$5 \cdot 10^8$ Hz range. At $\omega \to 0$

Table 1. The optimal set of the model parameters for the $K(H_{1-x}D_x)_2PO_4$ crystals.

x	T_c (K)	T_0 (K)	$\frac{\varepsilon}{k_B}$ (K)	$\frac{w}{k_B}$ (K)	$\frac{\nu_3(0)}{k_B}$ (K)	$\mu_{3-}, 10^{-18}$ $(esu \cdot cm)$	$\mu_{3+}, 10^{-18}$ $(esu \cdot cm)$	χ^0_{33}
0.00	122.5	122.5	56.00	422.0	17.91	1.46	1.71	0.73
0.81	205.6	204.8	85.82	781.5	33.44	1.76	2.02	0.42
1.00	220.1	219.0	93.05	868.6	35.76	1.84	2.10	0.34

x	$\frac{\psi_6}{k_B}$ (K)	$\frac{\delta_{s6}}{k_B}$ (K)	$\frac{\delta_{a6}}{k_B}$ (K)	$\frac{\delta_{16}}{k_B}$ (K)	$c^0_{66} \cdot 10^{-10}$ (dyn/cm^2)	e^0_{36} (esu/cm^2)	P_- (s)	R_- $(\frac{s}{K})$	P_+ (s)	R_+ $(\frac{s}{K})$
0.00	-150.00	82.00	-500.00	-400.00	7.10	1000.00	0.35	0.0100	0.43	0.0160
0.81	-200.00	52.73	-957.39	-400.00	6.45	1914.77	1.95	0.0082	4.19	0.0001
1.00	-138.64	45.64	-1068.18	-400.00	6.30	2136.36	2.84	0.0077	4.54	0.0349

we obtain a static dielectric permittivity of a free crystal. Taking into account the dispersion (3.12), we find the equation for the resonance frequencies

$$\omega_n = \frac{\pi(2n+1)}{l}\sqrt{\frac{c^E_{66}}{\rho}},$$

where taking into account the fact that in the $5 \cdot 10^5$–$5 \cdot 10^8$ Hz frequency range $c^E_{66}(\omega)$ is practically frequency independent. The resonance frequencies are inversely proportional to sample dimensions.

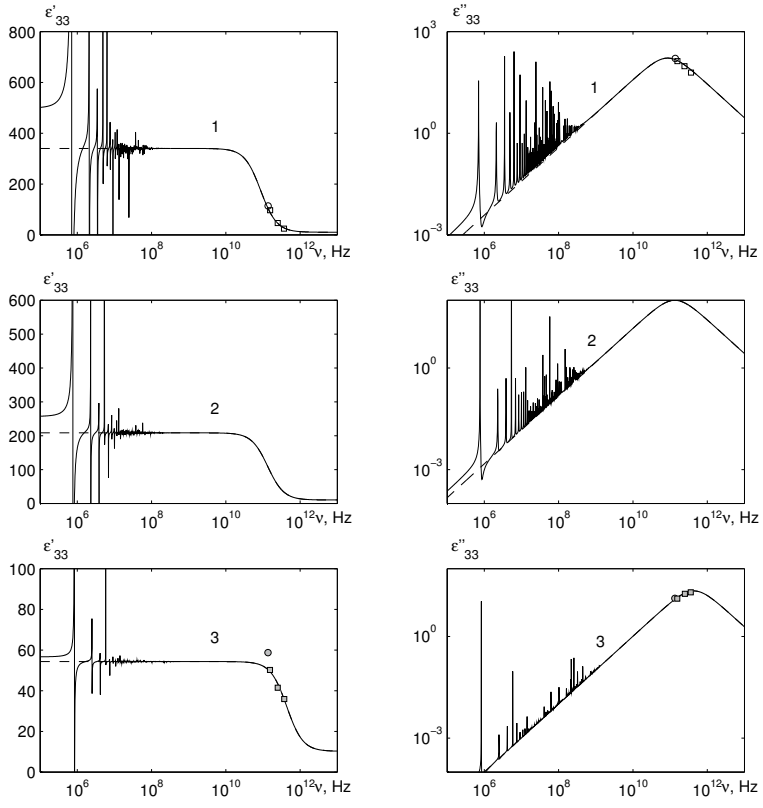

Figure 2. Frequency dependences of the real and imaginary parts of the dynamic dielectric permittivity of a mechanicallv free and clamped KH_2PO_4 crystal at different ΔT, K: 1 – 5, ○ [38], □ [39]; 2 – 10; 3 – 50 ● [38], ■ [39].

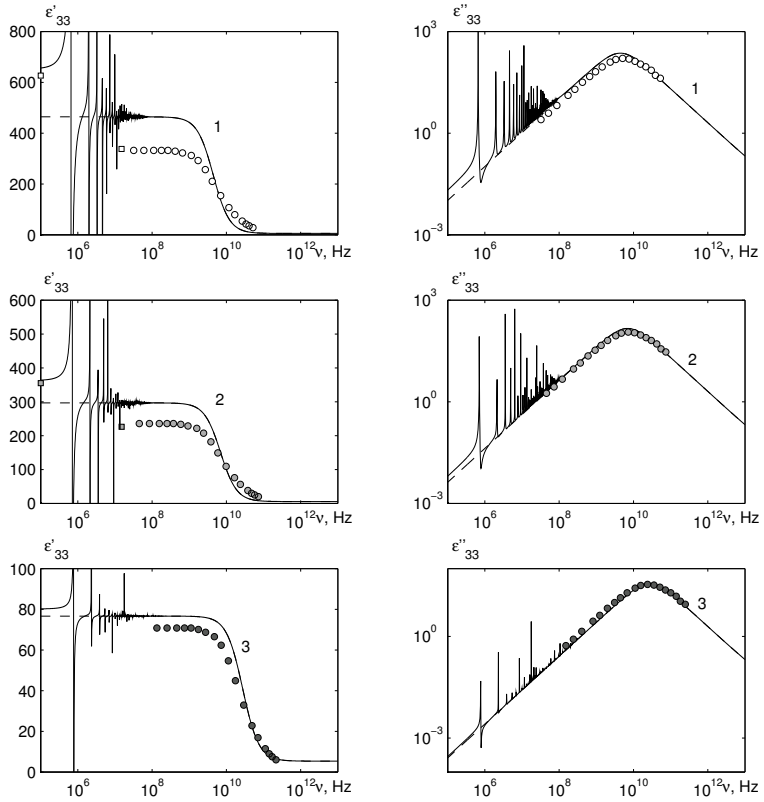

Figure 3. Frequency dependences of the real and imaginary parts of the dynamic dielectric permittivity of a mechanically free and clamped KD_2PO_4 crystal at different ΔT, K: 1 – 5, 2 – 10, 3 – 50. ○ , ● , ● [40].

The dashed lines in figures 2–3 describe the low-frequency permittivity of a clamped crystal. With increasing frequency and temperature ΔT, the amplitudes of the resonance peaks decrease. With increasing temperature ΔT the last resonance peak shifts to higher frequencies. Analogous multi-peak resonance dispersion is also observed in the ferroelectric phase. Above the resonance frequency, the crystal is clamped by the high-frequency field; above 10^9 Hz the clamped permittivity has a relaxational dispersion. The theoretical frequency curves $\varepsilon'_{33}(\omega)$ and $\varepsilon''_{33}(\omega)$ well accord with experimental data. The resonance dispersion in KH_2PO_4 is schematically presented in [43] for the ferroelectric phase at $10^4 - 10^6$ Hz.

In figure 4 we show the temperature curves of the real part $\varepsilon'_{33}(\omega, T)$ of the free dielectric permittivity of KH_2PO_4 at different frequencies. Below the frequency of the first resonance peak, the temperature variation of $\varepsilon^*_{33}(\omega, T)$ essentially coincides with that of the static permittivity of a free crystal. Near the resonance frequencies, the sharp peaks in the temperature curve of permittivity appear, the number of which increases with an increase of frequency, whereas the magnitudes decrease. Upon further increase of frequency, numerous resonance peaks of small amplitude arise around the curve of clamped permittivity. At even higher frequencies the peaks disappear. The resonance peaks for the real and imaginary parts of the permittivity for a given frequency are observed at the same temperature ΔT. The character of piezoelectric resonance curves is different for different crystals considered here.

In figure 5 we plot the calculated temperature dependences of the sound attenuation α_6 for KH_2PO_4, $K(H_{0,195}D_{0,805})_2PO_4$ at different frequencies along with the experimental points $\alpha_6(T)$ taken from [41,42]. A good quantitative description of experimental data is obtained, especially

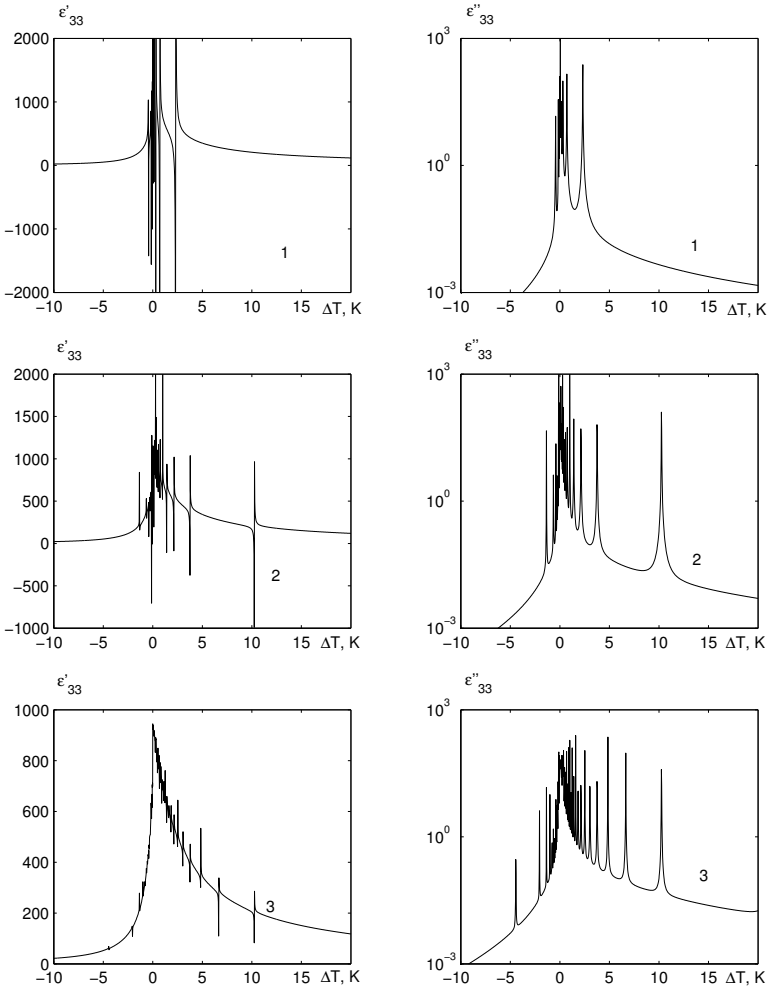

Figure 4. Temperature dependences of the real and imaginary parts of the dynamic dielectric permittivity of a mechanically free KH_2PO_4 crystal at different frequencies ν, MHz: 1 – 3, 2 – 10, 3 – 30.

for $K(H_{0.195}D_{0.805})_2PO_4$.

Near the transition temperature T_c, a sharp increase of attenuation is obtained. In the ferroelectric phase, the attenuation decreases much faster when moving away from the transition than in the paraelectric phase.

The dependence of attenuation α_6 on the square of frequency ω^2 for KH_2PO_4, $K(H_{0,195}D_{0,805})_2PO_4$ crystals at different temperatures ΔT is shown in figure 6. As one can see, attenuation varies proportionally to the square of frequency. The closer the temperature is to the Curie point, the larger is the rate of this variation.

With increasing frequency, starting from $\sim 10^7$ Hz, the theoretical attenuation sharply increases and then reaches a saturation at about 10^{10} Hz (figure 7). In the paraelectric phase, the cut-off frequency decreases with approaching the transition temperature T_c. The cut-off frequency also decreases with increasing deuteration x. Such high values of attenuation at saturation, in fact, mean the absence of sound propagation.

In figure 8 we depicted the calculated temperature dependence of sound velocity v_{66} for KH_2PO_4, $K(H_{0,195}D_{0,805})_2PO_4$.

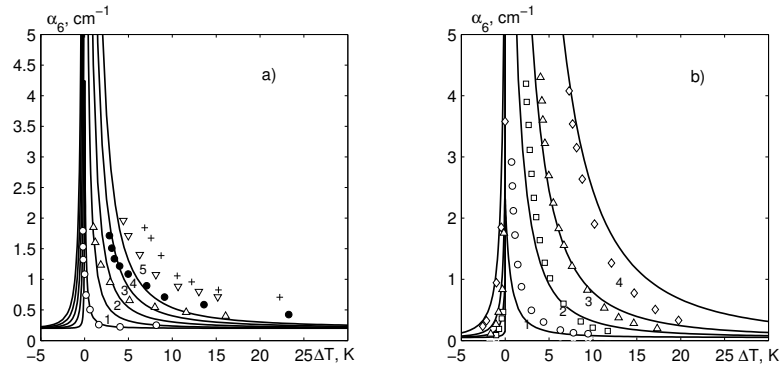

Figure 5. Temperature dependences of sound attenuation for KH_2PO_4 (a), at different frequencies $\nu, 10^6$ Hz: 1 – 10, ○ [41], 2 – 30, △ [41], 3 – 50, ● [41], 4 – 70, ▽ [41], 5 – 90,+[41] and $K(H_{0.195}D_{0.805})_2PO_4$ (b) at $\nu, 10^6$ Hz: 1 – 5, ○ [42], 2 – 15, □ [42], 3 – 25, △ [42], 4 – 45, ◇ [42].

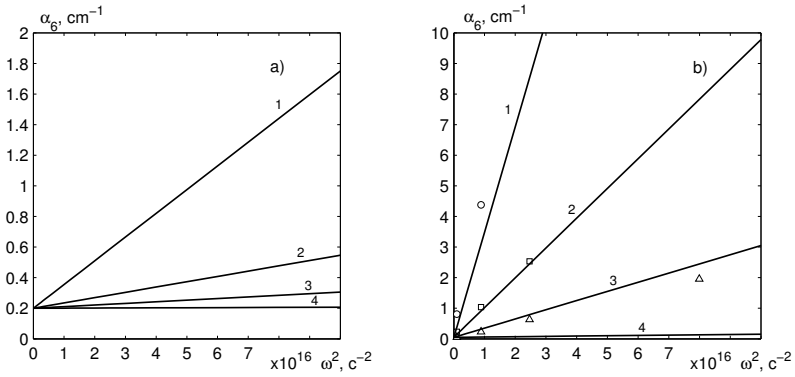

Figure 6. Frequency dependences of attenuation for KH_2PO_4 (a), $K(H_{0.195}D_{0.805})_2PO_4$ (b) at different temperatures ΔT,K: 1 – 2, 2 – 5, 3 – 10, 4 – 50. ○ , □ , △ – [42].

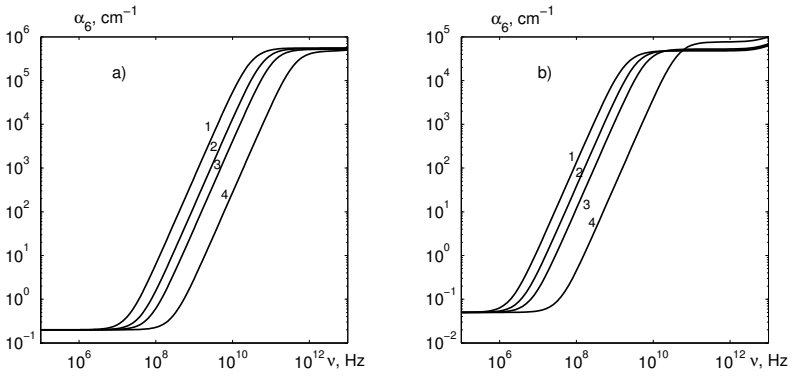

Figure 7. Frequency dependences of attenuation for KH_2PO_4 (a), $K(H_{0.195}D_{0.805})_2PO_4$ (b) at different temperatures ΔT,K: 1 – 2, 2 – 5, 3 – 10, 4 – 50.

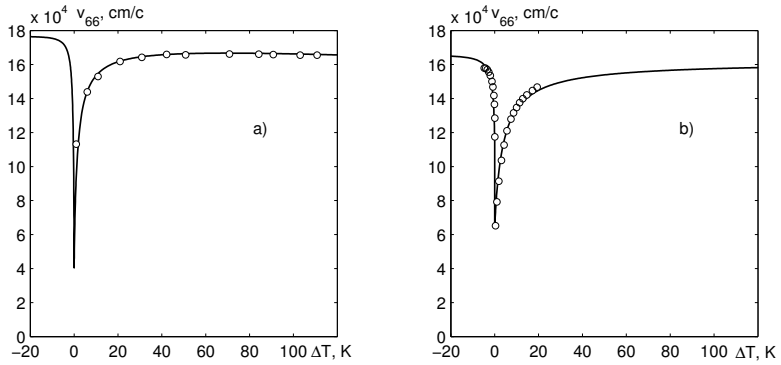

Figure 8. Temperature dependences of sound velocity for KH_2PO_4 (a), $K(H_{0.195}D_{0.805})_2PO_4$ (b).

It has a minimum at $T = T_c$. Below 10^{10} Hz, the magnitude of $c_{66}^E(\omega)$ is frequency independent; therefore, we calculated the velocity using (8.3) and experimental data for c_{66}^{TE} ([44] for KH_2PO_4 and [42] for $K(H_{0.195}D_{0.805})_2PO_4$) and crystal density ρ. The results are shown in figure 8 by symbols $\circ$.

At the frequency of microwave dispersion of permittivity, a sharp increase of sound velocity v_{66} should be observed, after which the frequency curve of velocity saturates at about $\sim 10^{11}$ Hz. The saturation values of sound velocity are temperature independent.

6. Conclusions

Within the proton ordering model with taking into account the shear strain ε_6 we explored a dynamic response of the KD_2PO_4 type crystals to an external harmonic electric field E_3. Dynamics of the pseudospin subsystem is described within the stochastic Glauber approach. Dynamics of the strain ε_6 is obtained from the Newtonian equations of motion of an elementary volume, with taking into account the relations between the order parameter of the pseudospin subsystem and the strain in the static limit. Expressions for the longitudinal dynamic dielectric permittivity of KD_2PO_4 crystals are obtained. Evolution of dynamic permittivity with increasing frequency via the piezoelectric resonances (10^5–10^8 Hz) to the clamped crystal with the microwave (10^9–10^{12} Hz) relaxational dispersion is obtained. Temperature and frequency dependences of sound attenuation α_6 and velocity v_{66} in $K(H_{1-x}D_x)_2PO_4$ are obtained. An anomalous increase of attenuation in the phase transition region and the temperature curve of sound velocity are described. A presence of cut-off frequency for sound propagation (an anomalous increase of attenuation at frequencies corresponding to the microwave dispersion of the dielectric permittivity) is predicted.

References

1. Blinc R., J. Phys. Chem. Solids, 1960, **13**, No. 3, 204.
2. De Gennes P.G., Solid State Commun., 1963, **1**, No. 6, 132.
3. Tokunaga M., Matsubara T., Progr. Theor. Phys., 1966, **35**, No. 4, 581.
4. Blinc R., Svetina S. Phys. Rev., 1966, **147**, No. 2, 430.
5. Stasyuk I.V., Levitskii R.R., Izv. AN SSSR, ser. fiz., 1971, **35**, No. 9, 1775 (in Russian).
6. Levitskii R.R., Korinevskii N.A., Stasyuk I.V., Ukr. Phys. J., 1974, **19**, No. 8, 1289 (in Russian).
7. Stasyuk I.V., Kaminskaya N.M., I. Ukr. Phys. J., 1974, **19**, No. 2, 237; II. Ukr. Phys. J., 1974, **19**, No. 2, 244.
8. Vaks V.G. Introduction into microscopic theory of ferroelectrics, Moskow, 1973 (in Russian).
9. Blinc R., Zeks B. Ferroelectrics and antiferroelectrics. Lattice dynamics. Moskow, 1975 (in Russian).
10. Vaks V.G., Zinenko V.I., Shneider V.E., Usp. Fiz. Nauk, 1983, **141**, No. 4(10), 629 (in Russian).

11. Stasyuk I.V. Doctoral thesis, Kiev, 1985.
12. Levitskii R.R. Doctoral thesis, Kiev, 1990.
13. Matsushita E., Matsubara T., J. Phys. Soc. Jpn., 1987, **56**, No. 1, 200.
14. Matsubara T., Jpn. J. Appl. Phys., 1985, **24**, Suppl. 24-2, 1.
15. Levitsky R.R., Zachek I.R., Vdovych A.S. Preprint of the Institute for Condensed Matter Physics, ICMP–08–04U, Lviv, 2008 (in Ukrainian).
16. Glauber J., J. Math. Phys., 1963, **4**, No. 2, 294.
17. Yoshimitsu K., Matsubara T., Suppl. Progr. Theor. Phys., 1968, 109.
18. Levitsky R.R., Zachek I.R. Preprint of the Bogolyubov Institute for Theoretical Physics, ITP-77-29R, Kyiv, 1977 (in Russian).
19. Levitsky R.R., Zachek I.R. Preprint of the Bogolyubov Institute for Theoretical Physics, ITP-77-30R, Kyiv, 1977 (in Russian).
20. Levitsky R.R., Zachek I.R., Varanitsky V.I. Preprint of the Bogolyubov Institute for Theoretical Physics, ITP-79-11E, Kiev, 1979.
21. Zachek I.R., Levitsky R.R., Teor. Mat. Fiz., 1980, **43**, No. 1, 128 (in Russian).
22. Levitsky R.R., Zachek I.R., Varanitsky V.I., Ukr. Phys. J., 1980, **25**, No. 12, 1961 (in Russian).
23. Levitsky R.R., Zachek I.R., Mits Ye.V. Preprint of the Bogolyubov Institute for Theoretical Physics, ITP-87-114R, Kyiv, 1987 (in Russian).
24. Levitsky R.R., Zachek I.R., Mits Ye.V. Preprint of the Bogolyubov Institute for Theoretical Physics, ITP-87-115R, Kyiv, 1987 (in Russian).
25. Zachek I.R., Mits Ye.V., Levitsky R.R. Preprint of the Bogolyubov Institute for Theoretical Physics, ITP-89-7R, Kyiv, 1987 (in Russian).
26. Stasyuk I.V., Levitskii R.R., Korinevskii N.A., Phys. Status Solidi B, 1979, **91**,No. 2, 541.
27. Levitskii R.R., Stasyuk I.V., Korinevsky H.A., Ferroelectrics, 1978, **21**, 481.
28. Korinevskii N.A., Levitskii R.R., Teor. Mat. Fiz., 1980, **42**, No. 3, 416 (in Russian).
29. Yomosa Sh., Nagamiya T., Progr. Theor. Phys., 1949, **4**, No. 3, 263.
30. Slater J.C., J. Chem. Phys., 1941, **9**, No. 1, 16.
31. Stasyuk I.V., Biletskii I.N. Preprint of the Bogolyubov Institute for Theoretical Physics, ITP-83-93R, Kyiv, 1983 (in Russian).
32. Stasyuk I.V., Biletskii I.N., Styagar O.N., Ukr. Phys. J., 1986, **31**, No. 4, 567.
33. Stasyuk I.V., Levitskii R.R., Zachek I.R., Moina A.P., Phys. Rev. B, 2000, **62**, No. . 10, 6198.
34. Stasyuk I.V., Levitskii R.R., Moina A.P., Lisnii B.M., Ferroelectrics, 2001, **254**, 213.
35. Levitskii R.R., Lisnii B.M., Phys. Status Solidi B, 2004, **241**, No. 6, 1350.
36. Levitskii R.R., Zachek I.R., Vdovych A.S. Preprint of the Institute for Condensed Matter Physics, ICMP-06-08U, Lviv, 2006 (in Ukrainian).
37. Moina A.P. Levitskii R.R., Zachek I.R., Phys. Rev. B, 2005, **71**, 134108.
38. Gauss K.E., Happ H., Rother G., Phys. Status Solidi B, 1975, **72**, No. 2, 623.
39. Volkov A.A., Kozlov G.V., Lebedev S.P., Velychko I.A., Fiz. Tverd. Tela, 1979, **21**, No. 11, 3304 (in Russian).
40. Hill R.M., Ichiki S.K., Phys. Rev., 1963, **130**, No. 1, 150.
41. Litov E., Garland C.M., Phys. Rev. B, 1970, **2**, No. 11, 4597.
42. Litov E., Uehling E.A., Phys. Rev. B, 1970, **1**, No. 9, 3713.
43. Poplavko Y.M. Mechanisms of electrical relaxation in the order-disorder type ferroelectrics (ODF). – In: Mechanisms of relaxation fenomena in solids, Kaunas, 1974 (in Russian).
44. Mason W. Piezoelectric crystals and its application in ultraacoustics, Moskow, 1952 (in Russian).

Поздовжня релаксація механічно вільних кристалів типу KH_2PO_4. П'єзоелектричний резонанс та поглинання звуку

Р.Р.Левицький[1], І.Р.Зачек[2], А.С.Моїна[1], А.С.Вдович[1]

[1] Інститут фізики конденсованих систем НАН України, 79011 Львів, вул. Свєнціцького 1

[2] Національний університет "Львівська політехніка", 79013 Львів, вул. С. Бандери 12

Отримано 5 червня 2008 р., в остаточному вигляді – 9 липня 2008 р.

В рамках протонної моделі з врахуванням п'єзоелектричної взаємодії зі зсувною деформацією ε_6 розглянуто динамічний діелектричний відгук сегнетоелектриків типу KD_2PO_4. Враховано динаміку п'єзоелектричної деформації. Явно описано явища затискання кристалу високочастотним електричним полем, п'єзоелектричного резонансу і НВЧ дисперсії, що спостерігаються на експерименті. Розраховано коефіцієнт поглинання звуку. Описано особливості коефіцієнта поглинання в околі точок переходу. Передбачено наявність обрізаючої частоти у частотній залежності коефіцієнта поглинання звуку.

Ключові слова: *сегнетоелектрики, п'єзоелектричний резонанс*

PACS: *77.22.Ch, 77.22.Gm, 77.65.-j, 77.84.Fa, 77.65.Fs*